Force Kinetics and Individual Sarcomere Dynamics in Cardiac Myofibrils after Rapid Ca^{2+} Changes

R. Stehle, M. Krüger, and G. Pfitzer
Institute of Physiology, University Cologne, D-50931 Köln, Germany

ABSTRACT Kinetics of force development and relaxation after rapid application and removal of Ca^{2+} were measured by atomic force cantilevers on subcellular bundles of myofibrils prepared from guinea pig left ventricles. Changes in the structure of individual sarcomeres were simultaneously recorded by video microscopy. Upon Ca^{2+} application, force developed with an exponential rate constant k_{ACT} almost identical to k_{TR}, the rate constant of force redevelopment measured during steady-state Ca^{2+} activation; this indicates that k_{ACT} reflects isometric cross-bridge turnover kinetics. The kinetics of force relaxation after sudden Ca^{2+} removal were markedly biphasic. An initial slow linear decline (rate constant k_{LIN}) lasting for a time t_{LIN} was abruptly followed by an ~20 times faster exponential decay (rate constant k_{REL}). k_{LIN} is similar to k_{TR} measured at low activating [Ca^{2+}], indicating that k_{LIN} reflects isometric cross-bridge turnover kinetics under relaxed-like conditions (see also Tesi et al., 2002. *Biophys. J.* 83:2142–2151). Video microscopy revealed the following: invariably at t_{LIN} a single sarcomere suddenly lengthened and returned to a relaxed-type structure. Originating from this sarcomere, structural relaxation propagated from one sarcomere to the next. Propagated sarcomeric relaxation, along with effects of stretch and P_i on relaxation kinetics, supports an intersarcomeric chemomechanical coupling mechanism for rapid striated muscle relaxation in which cross-bridges conserve chemical energy by strain-induced rebinding of P_i.

INTRODUCTION

Repeated cycles of Ca^{2+}-activated myofibrillar contraction and relaxation underlie the mechanical performance of heartbeats. Cross-bridges are the force-generating motors behind the contractions. To obtain insight about the cross-bridge kinetics during an activation-relaxation cycle, studies of flash photolysis of caged Ca^{2+} and caged Ca^{2+} chelators have been carried out on skinned cellular (Araujo and Walker, 1994, 1996) and multicellular heart muscle preparations (Zhang et al., 1995; Palmer and Kentish, 1997, 1998; Simnett et al., 1998; Fitzsimons et al., 1998; Johns et al., 1997, 1998, 1999; Kentish et al., 2001). It was found that, upon Ca^{2+} removal, isometric force decays as fast as or faster than it develops upon Ca^{2+} application (Palmer and Kentish, 1998). Models, however, predict that the turnover kinetics of cross-bridges are slower during relaxation than during activation (Huxley, 1957; Brenner, 1988). This raised questions about the origin of the rapid cross-bridge kinetics after Ca^{2+} removal, not only of cardiac muscle (Palmer and Kentish, 1998) but also of skeletal muscle (Hoskins et al., 1999). Early studies of post-tetanic relaxation in living skeletal muscle fibers revealed large changes of fiber segment length and of mean sarcomere length (SL) that begin at the onset of the final rapid force decay (Huxley and Simmons, 1970; Edman and Flitney, 1982). The rapid fall in tension was interpreted to arise from the give of sarcomeres at the ends of the fiber causing rapid cross-bridge detachment (Huxley and Simmons, 1970). However, it is uncertain whether inhomogeneous relaxation of sarcomeres in intact fibers is caused by inhomogeneous uptake of Ca^{2+} into intracellular stores (Edman and Flitney, 1982; Hoskins et al., 1999) or whether it reflects an intrinsic contractile property of the sarcomere. Furthermore, there is no information about relaxation on the single-sarcomere level. Clearly, if length changes occur during relaxation on the level of individual sarcomeres in the isolated myofibrillar structure, it is evident that cross-bridge kinetics would be basically affected by the filament sliding even though the preparation is held isometric.

In the experiments described here, force changes were correlated with the length of individual sarcomeres during tension development and relaxation induced by near instantaneous changes in [Ca^{2+}]. Myofibrils are ideal for this type of investigation. Their architecture consists of a limited number of sarcomeres, which allows to follow the behavior of each individual sarcomere (Anazawa et al., 1992; Linke et al., 1993). The short diffusion distances in myofibrils ensure rapid equilibration with the surrounding solution. We adapted the rapid solution change technique developed by Poggesi and coworkers (Colomo et al., 1998) to an apparatus that measures myofibrillar force by an atomic force cantilever. The displacement of the atomic force cantilever is detected by an external laser beam, which is independent of the microscope optics. This enables simultaneous recording of force transients and phase contrast video images from which length changes of individual sarcomeres can be analyzed.

We previously demonstrated that rapid Ca^{2+} removal from isometrically contracting cardiac myofibrils induces markedly biphasic force decays (Stehle et al., 2002). Here, we elucidate the origin and the relation to cross-bridge

Submitted January 16, 2002, and accepted for publication June 13, 2002.
Address reprint requests to Dr. R. Stehle, Institute of Physiology, University Cologne, Robert-Koch-Strasse 39, D-50931 Köln, Germany. Tel.: 49-221-4786952;, Fax: 49-221-4786965; E-mail: Robert.Stehle@Uni-Koeln.de.

0006-3495/02/10/2152/10 $2.00

kinetics of the two distinct phases of relaxation by investigating force kinetics and sarcomere behavior during relaxation and comparing them with those measured during activation. We then tested whether the strain generated in the sarcomeres during contraction can be reconverted to chemical energy during relaxation by the reversal of the cross-bridge power stroke.

MATERIAL AND METHODS

Myofibrillar preparation and solutions

Myofibrils were prepared from left ventricles of the guinea pig as described in a previous paper (Stehle et al., 2002). Standard relaxing/activating solution contained either 3 mM K_4Cl_2Ca-EGTA (activating) or 3 mM K_4Cl_2-EGTA (relaxing solution), 10 mM imidazole, 1 mM $K_2Cl_2Na_2$Mg-ATP, 3 mM $MgCl_2$, 47.7 mM Na_2CrP, 2 mM dithiothreitol, pH 7.0, at 10°C; final ionic strength (μ) = 0.17 M. The concentration of P_i was measured by an assay kit (E-6646, Molecular Probes, Eugene, OR). The P_i contamination in standard solutions was 190 ± 30 μM (mean ± SD). Solutions containing less P_i were produced by adding 1 mM methylguanosine and 0.5 U/ml purine nucleotide phosphorylase, resulting in 15 ± 4 μM free P_i. To produce solutions with higher [P_i] of the same ionic strength, Na_2CrP was replaced by P_i in a molar ratio of 2:3.

Apparatus and experiments

On a rigid stage of an Olympus IX-70 microscope all manipulators holding the chamber, the microtools, the laser, and the detector were mounted. The force signal was obtained by microfocusing a single-mode coupled laser beam with a 20-μm spot size onto the back of a force modulation etched silicon probe-type atomic force cantilever (Nanosensors, Wetzlar-Blankenfeld, Germany) and then detecting the displacement of the reflected beam by a detector (SPOT-9D, Polytec, Waldbronn, Germany) with an effective amplification (displacement of laser on detector per cantilever displacement) of ~2300. The cantilevers used here have improved performance: 5–50 times higher resonance frequency (~25 kHz in solution) and 5–10 times higher stiffness (2–4 μN/μm), compared with the microneedles used previously to measure myofibril force (Cecchi et al., 1993; Fearn et al., 1993). This improved performance allowed for highly time-resolved, isometric measurements.

A droplet of myofibrillar suspension was placed in the chamber filled with relaxing solution thermostated to 10°C. Bundles containing one to six myofibrils were stuck at their ends to 1) the tip of a stiff tungsten needle (5775, A-M Systems, Carlsborg, WA) that was motored by a piezoactuator (P-821.20, Physik Instruments, Karlsruhe, Germany) to act as a length driver and 2) a cantilever tip that had been precoated with a mixture (1:3 v/v) of silicon glue (3140 RTV Coating, Dow Corning, Midland, MI) and 2% nitrocellulose in amylacetate. Myofibril dimensions were determined, and video microscopy was performed under phase contrast using either a CellCam color camera (Phase, Lübeck, Germany) or an ORCA-ER camera (Photonics, Hamamatsu City, Japan). Single myofibrils were 1.1 ± 0.2 μm in width and 25–40 μm in length; bundles were ≤3 μm in width and 40–110 μm in length. Slack SL was 1.98 ± 0.04 μm (mean ± SD). Before activation, myofibrils were prestretched to a SL of 2.25–2.4 μm. The principle of rapid solution change was as described by Colomo et al. (1998): two continuous laminar streams, one containing relaxing solution, the other activating solution, were applied by gravitation pressure perpendicular to the myofibril through a pulled and microforge-bent θ-style capillary (TGC150–15, Clark Electromedical Instruments, Reading, UK). The capillary was preadjusted to fully expose the myofibril to the stream of relaxing solution. For activation/relaxation, the capillary was moved rapidly by a piezoactuator (P289.40, Physik Instruments). The time that elapsed from the capillary movement to the effective solution change at the myofibril (dead time) was indicated by a single peak-like or sinusoidal-like artifact in the force signal that resulted from transient deflections of the laser beam. Video microscopy of flow profiles (Stehle et al., 2002) confirmed that this artifact lasts during the time the flow profile at the cantilever is bent, i.e., during the time the solution interface passes the myofibril. The delay of the artifact (5–30 ms) depended on the flow rate adjusted by gravitation (20–50 cm H_20) and the distance from the pipette tip to the myofibril (0.3–0.7 mm). The period of the artifact was similar (±20%) to the adjustable time of actuator movement, which was set to 10–20 ms.

Data acquisition and analysis

Signal conditioning for movement of actuators, acquisition of force and length signals, determination of individual and/or mean SL, and kinetic analysis of force transients were performed with a PCI6110-E device and self-written programs in LabView 4.0 (National Instruments, Austin, TX). To determine k_{ACT} or k_{TR}, single exponentials (e.g., see Fig. 4 *A*) were fitted to the transients by defining $t = 0$ for the fits at the end of the artifacts described above. Similarly, to determine k_{LIN}, t_{LIN}, and k_{REL}, a function consisting of a linear and an exponential term (Stehle et al., 2002; e.g., see Fig. 4 *B*) was fitted to the transients. Video images were quantitatively analyzed by selecting a rectangular region of interest and integrating pixel intensities to an intensity profile in AquaCosmos 1.3.0.1 (Hamamatsu Photonics). Individual SL and mean SL values were then determined from the profiles using the LabView built-in files (virtual instruments) peak detector.vi and power spectrum.vi, respectively.

RESULTS

The average active force developed by cardiac myofibrils at 10°C in standard solutions (see Materials and Methods) was 149 ± 16 nN/μm^2 (mean ± SE; n = 36). This is similar to values reported for frog atrial myocytes (149 nN/μm^2 at 15°C (Colomo et al., 1997)) and to an earlier report for single mammalian cardiac myofibrils (145 nN/μm^2 at 20°C (Linke et al., 1994)). Myofibrils were fully Ca^{2+} regulated as indicated by their low resting tension (≤5% of maximum Ca^{2+}-activated force at SL ≤ 2.4 μm) in relaxing solution. The pCa required for half-maximal force generation and the Hill slope (*nH*) of force-pCa relations (n = 12) averaged 5.57 ± 0.03 and 3.8 ± 1.1, respectively.

Fig. 1 *A* shows force transients upon switching from pCa 7.5 to pCa 4.5 and back to pCa 7.5 (myofibrillar bundle under standard conditions). Force development can be fitted by a single exponential (rate constant k_{ACT}), whereas force decay is best described by two phases (magnified in Fig. 1 *B*): an initial slow linear decline of duration t_{LIN} (and a rate constant k_{LIN} which is determined from the slope of the slow linear decline normalized to the amplitude of the overall force decay) is followed by a rapid exponential decay (rate constant k_{REL}). The means of the kinetic parameters are given in Table 1. The initial, slow, linear force decay is not due to slow Ca^{2+} removal, because t_{LIN} is strongly reduced by increasing the temperature and by increasing [P_i] (cf. Table 1). We previously showed that these shapes in the force kinetics, i.e., monophasic exponential

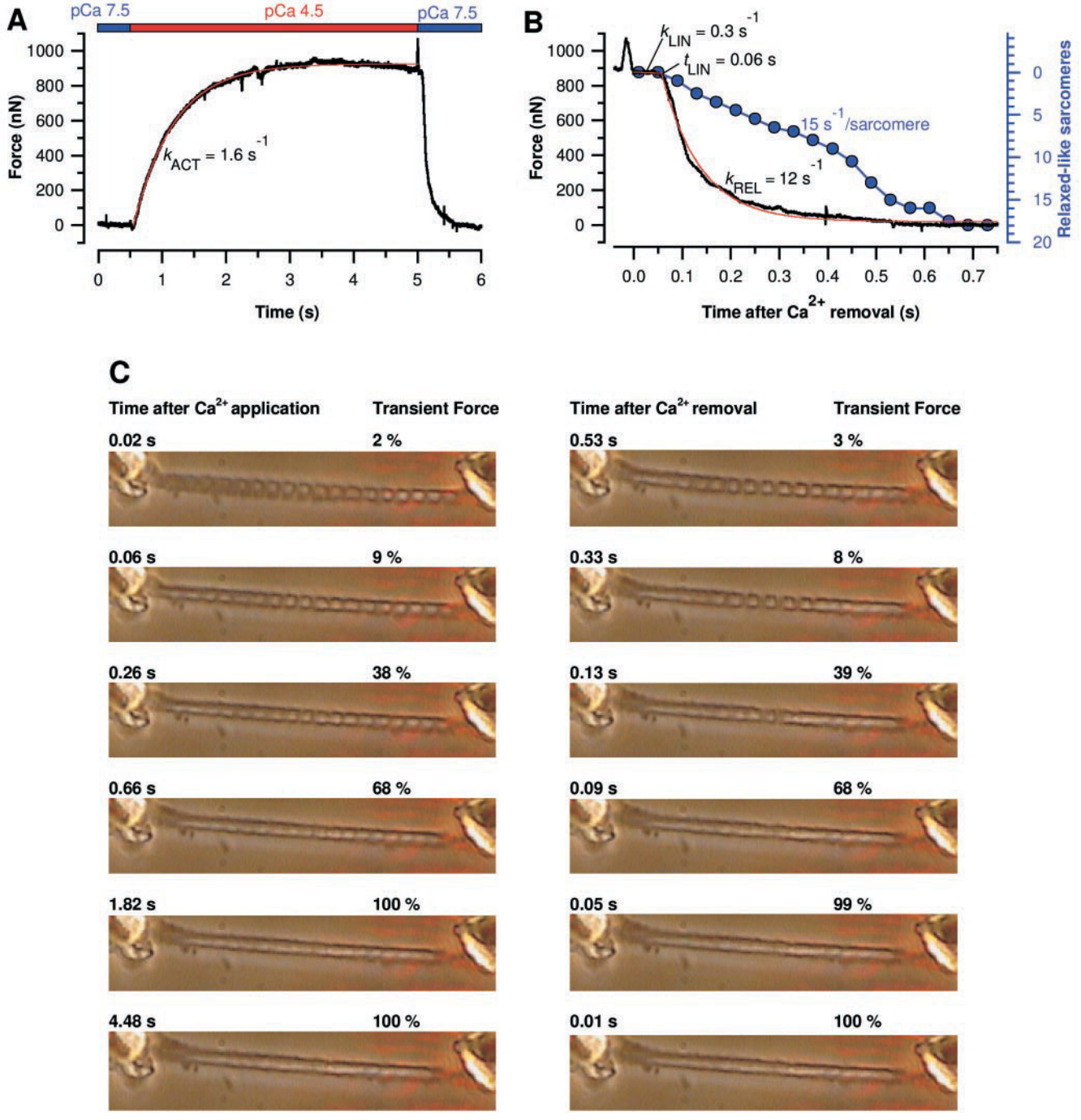

FIGURE 1 Force kinetics and sarcomere dynamics during a contraction-relaxation cycle of a myofibrillar bundle (18 sarcomeres; force per cross-sectional area calculated from the mean diameter of 2.6 μm = 180 nN/μm^2) from guinea pig left ventricle at 10°C. (*A*) Kinetics of force development upon Ca^{2+} application. (*B*) Kinetics of force decay upon Ca^{2+} removal on an expanded time scale plotted together with the number of stretched, relaxed-like sarcomeres (*blue symbols*) developing over time, as determined from images of the type shown in *C*, sampled in 40-ms intervals. Red lines in *A* and *B* are best fits to force transients (*black lines*) giving the kinetic parameters indicated. (*C*) Phase contrast micrographs recorded at the times indicated after Ca^{2+} application (*left panel*, *top to bottom*) and after Ca^{2+} removal (*right panel, bottom to top*). The images shown were selected and arranged side by side to illustrate the different sarcomere patterns observed during force development and force decay under similar transient force levels, indicated by the values of relative force (related to maximum force) next to each image.

force development and biphasic force relaxation, are found ubiquitously in cardiac myofibrils from various species (Stehle et al., 2002).

To obtain insight into the origin of the biphasic nature of relaxation, sarcomeres were imaged by video microscopy (Fig. 1 *C*) while recording the force transients shown in Fig.

TABLE 1 Effect of activating [Ca^{2+}], P_i, and *T* on myofibrillar force kinetic parameters

Conditions*	Force†	k_{ACT} (s^{-1})	k_{TR} (s^{-1})	k_{LIN} (s^{-1})	t_{LIN} (ms)	k_{REL} (s^{-1})
Standard	1.00 (32)	1.62 ± 0.08 (32)	1.52 ± 0.12 (15)	0.66 ± 0.07 (32)	109 ± 5 (32)	10.9 ± 0.4 (32)
pCa 5.88	0.17 ± 0.08 (12)	0.51 ± 0.05 (12)	0.53 ± 0.13 (7)	0.58 ± 0.21 (10)	49 ± 7 (12)	4.9 ± 0.6 (12)
15 μM P_i	1.09 ± 0.03 (8)	1.68 ± 0.12 (8)	1.70 ± 0.20 (4)	0.70 ± 0.19 (8)	151 ± 23 (8)	11.1 ± 1.0 (8)
5 mM P_i	0.68 ± 0.03 (9)	2.36 ± 0.14 (9)	3.06 ± 0.38 (4)	1.91 ± 0.50 (7)	24 ± 5 (7)	18.7 ± 2.3 (7)
20 mM P_i	0.39 ± 0.02 (13)	3.95 ± 0.30 (13)	5.11 ± 0.65 (6)	ND	7 ± 2 (11)	23.3 ± 2.7 (11)
23°C	1.62 ± 0.09 (11)	7.2 ± 0.6 (11)	6.8 ± 0.9 (7)	3.6 ± 0.5 (11)	28 ± 3 (11)	27.3 ± 1.7 (11)

ND, not done.
*Conditions, unless otherwise indicated, refer to standard conditions: activating pCa = 4.5, [P_i] = 0.2 mM, and T = 10°C. Values are means ± SE (n).
†Ca^{2+}-activated force was normalized to standard conditions.

1, *A* and *B*. Throughout force development, sarcomeres in the middle of the bundle shortened (on average by 9 ± 4%; seven videos), presumably because of end compliance. However, no organized lengthening or shortening of individual sarcomeres could be detected. The contrast between sarcomeric bands decreased, not only because of I-band shortening but also because of decreased sharpness in A-bands and I-bands. During relaxation, no movements of the sarcomeres were detected in the first two images, which were collected 10 ms and 50 ms after the Ca^{2+} removal. However, in the first image taken after initiation of the rapid exponential force decay (t = 90 ms), a single sarcomere started to lengthen (in this example, in the middle of the myofibril). In the following image (t = 130 ms), its lengthening was completed, and it assumed the contrast of a relaxed sarcomere. Starting from this sarcomere, lengthened sarcomeres successively appeared in both directions with similar speeds of propagation. Fig. 1 *B* shows the number of sarcomeres reassuming a typical relaxed appearance with time. Whereas the propagation of relaxation from sarcomere to sarcomere is rapid (mean rate ≈ 15 s^{-1} per sarcomere in one direction), the overall structural relaxation takes much longer to decay than force does.

The sarcomere behavior after Ca^{2+} removal (shown in Fig. 1 *C*) is observed in every video we collected under all conditions (Table 1); i.e., 1) lengthening of the first sarcomere starts at t_{LIN} within the time error given by the interval of image sampling (20–40 ms) and 2) lengthening propagates sequentially from sarcomere to sarcomere during and still after the exponential force decay. Lengthening started preferentially in rather long sarcomeres but never directly at the attached ends. In those bundles in which the homogeneity of sarcomeres was most preserved, which one of the sarcomeres that lengthened first could change, depending on which ones became the longest sarcomeres at the end of the preceding Ca^{2+} activation. The formation of relaxed sarcomeres and their systematic propagation are not a result of inhomogeneous deactivation arising from Ca^{2+} gradients in the solution flow, because 1) sarcomeres contract simultaneously during Ca^{2+} activation and 2) force kinetics were unaffected by changing the Ca^{2+}-buffering capacity in activating or relaxing solutions (Stehle et al., 2002). Instead, the reason that lengthening initiates at a certain sarcomere seems to be that it is mechanically weak.

Fig. 2 shows an example of quantitative length changes occurring in individual sarcomeres after rapid Ca^{2+} removal. In addition to illustrating the most pronounced lengthening of sarcomeres, the figure also shows some other typical observations. 1) Sarcomeres that lengthen early in a propagation are stretched beyond their resting SL, presumably because of the strain exerted by the still contracting sarcomeres. 2) Sarcomeres that lengthen later on in a prop-

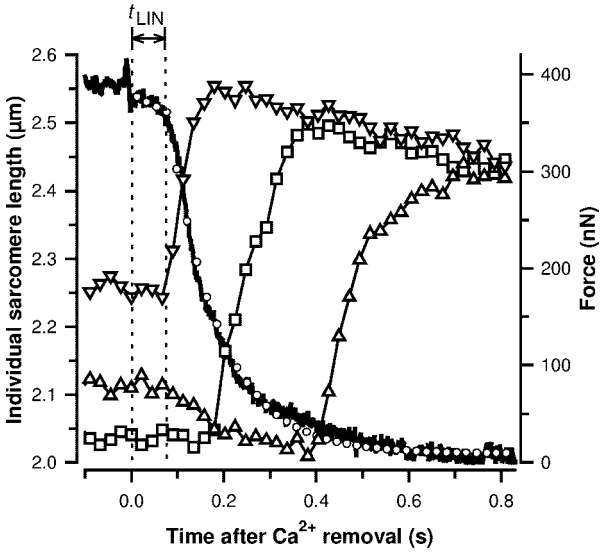

FIGURE 2 Length changes in individual sarcomeres and force decay after rapid Ca^{2+} removal. A myofibril bundle consisting of 16 sarcomeres (mean resting SL, 2.41 μm; SD of individual resting SL, ±0.05 μm) was activated at pCa 4.5 for 5 s after which mean SL decreased to 2.15 μm and SD of individual SL increased to ±0.16 μm. Then, the pCa was reduced to 7.5 at t = 0 indicated in the figure. For clarity, only the SL changes of three exemplary sarcomeres are shown: the first (▽), the fourth (○), and the seventh (□) sarcomere starting to lengthen in one direction of the propagation. Lengthening initiated near the middle of the myofibril. The seventh sarcomere (□) was equal to the second to last lengthening sarcomere. The small circles superimposed on the force transient indicate its best fit, giving the parameters k_{LIN} = 0.7 s^{-1}, t_{LIN} = 0.078 s, and k_{REL} = 9.2 s^{-1}. Note that the SL of the first sarcomere (▽) starts to significantly increase at the data point evaluated from the first video image sampled after t_{LIN}.

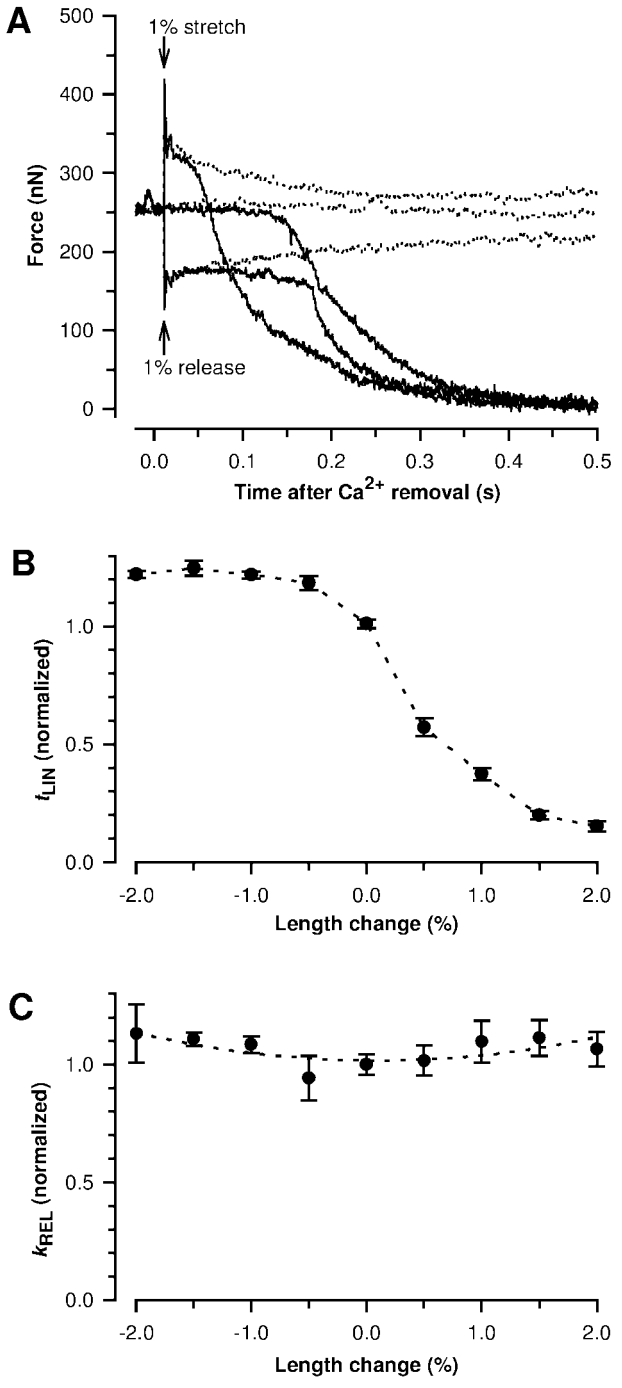

FIGURE 3 Effect of small rapid length changes on cardiac myofibrillar relaxation kinetics. (*A*) Force transients after step changes of 1% in myofibrillar length applied to cardiac myofibrils at steady-state Ca^{2+} activation (*dotted transients*) or 10 ms after the Ca^{2+} removal (*continuous transients*). Transients that sharply increase or decrease at $t = 10$ ms show a response to rapid stretch or rapid release, respectively. Transients without changes at $t = 10$ ms are the isometric controls. (*B*) Dependence of the time of the tension shoulder (t_{LIN}) on the amplitude of the length steps (positive values are stretches; negative values are releases). (*C*) Dependence of the rate constant of the exponential decay, k_{REL}, on the amplitude of the length steps. In *B* and *C*, the data of seven bundles are summarized (error bars represent SE). For each bundle, the data of t_{LIN} and k_{REL} were normalized to their value at isometric conditions and then averaged. The stretch amplitude that reduces t_{LIN} to 50% of its value at isometric conditions, as estimated by interpolating the individual relation of each bundle, averaged 0.61 ± 0.04% of myofibrillar length, relating to 7.2 ± 0.5 nm/half-sarcomere (mean ± SE).

agation shorten (presumably actively) after the onset of the rapid force decay preceding their lengthening. 3) sarcomeres which had completed lengthening all adopt very similar lengths; i.e., among the lengthened sarcomeres the SL becomes very homogeneous, which is a typical feature of relaxed sarcomeres and suggests that the lengthened sarcomeres are already fully relaxed while the other sarcomeres are still contracting.

Quantitative analysis of individual SL from images of seven videos revealed the following (not illustrated): at the time when the first three sarcomeres in a myofibril had lengthened to 2.55 ± 0.08 μm (mean ± SD), force had dropped to 25 ± 3% of its initial value. This is lower than the dynamic passive force at 2.55 μm SL (32 ± 4% of Ca^{2+}-activated force), which was measured by stretching myofibrils from slack SL, in relaxing solution, with about the same speed (~4 μm/s per sarcomere) at which the lengthening of individual sarcomeres after Ca^{2+} removal had occurred. This is consistent with the idea that the sarcomeres that became lengthened behave mechanically as being fully relaxed. We therefore call the lengthened sarcomeres relaxed and the others contracting, but note that this refers to their structural and mechanical properties, not to their state of activation.

Because the final mechanical relaxation of individual sarcomeres begins when they lengthen, the effect of myofibrillar length changes on relaxation kinetics was investigated. Fig. 3 *A* shows that rapidly stretching a bundle shortly after the Ca^{2+} removal resulted in a transient tension with initial phases (T_1 and T_2) similar to those observed after applying such a stretch at steady-state Ca^{2+} activation. However, stretching the bundle after Ca^{2+} removal caused the rapid exponential force decay to start much earlier than under isometric conditions. Rapid releases slightly increased t_{LIN}. Videos collected during this type of experiment (not shown) reveal that 1) length steps first distribute homogeneously to all the sarcomeres and 2) systematic sarcomere dynamics of the type described for Figs. 1 and 2 initiated, as usual, at the time of the tension shoulders (t_{LIN}). The dependences of t_{LIN} and k_{REL} on the amplitude of the length change are shown in Fig. 3, *B* and *C*, respectively. Whereas k_{REL} is not much affected by either stretches or releases, t_{LIN} is halved by stretching bundles ~7 nm per half-sarcomere (Fig. 3 *B*). This suggests that straining cross-bridges in a half-sarcomere by 7 nm, or even by less if taking filament compliance into account (Piazzesi et al., 1997), induces the rapid final relaxation of an individual sarcomere.

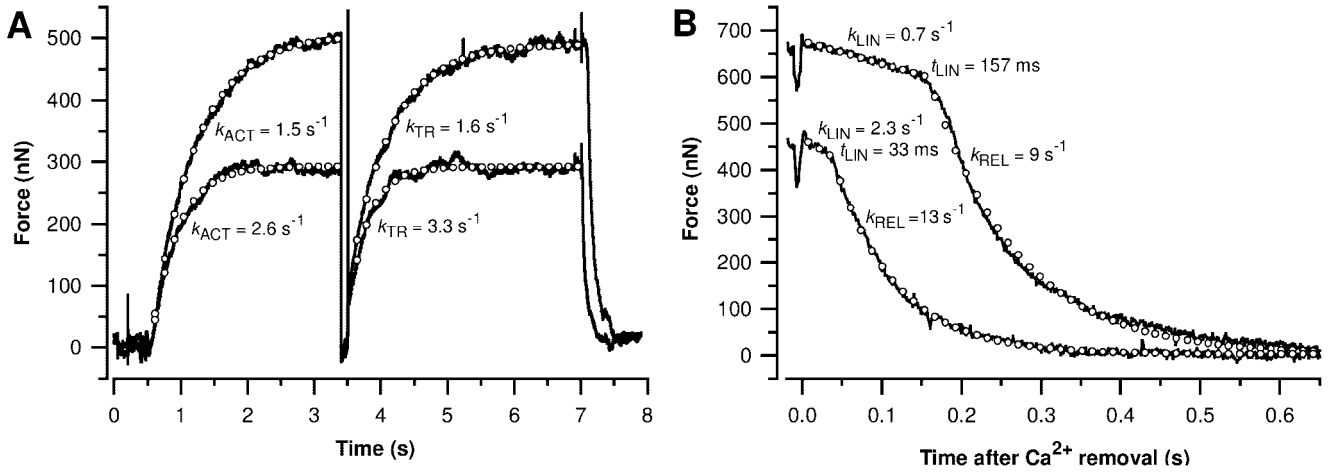

FIGURE 4 Effect of P_i on myofibrillar force kinetics. Upper transients were recorded at standard conditions (the activating and relaxing solutions each contained 0.2 mM P_i); lower transients were recorded in the presence of 5 mM P_i added to both solutions. The small circles indicate the fits to the transients, giving the values of kinetic parameters indicated. (*A*) Ca^{2+}-induced force development (switching from pCa 7.5 to pCa 4.5 at $t = 0.5$ s) and force redevelopment during steady-state Ca^{2+} activation at pCa 4.5 (starting at $t = 3.5$ s) after a period of active unloaded shortening induced by a release-restretch maneuver (amplitude, 15% of l_0; duration, 100 ms). Ca^{2+} is removed (switching from pCa 4.5 to pCa 7.5) at $t = 7$ s. (*B*) Force decays after a switch from pCa 4.5 to pCa 7.5 of a different bundle as in *A*.

A basic feature of most cross-bridge models (e.g., Eisenberg et al., 1980; Pate and Cooke, 1989; Rayment et al., 1993) is that cross-bridges generate force, i.e., strain, by a power stroke that is closely associated with the reversible release of P_i, though not necessarily directly (Millar and Homsher, 1990). Vice versa, as predicted by some models (Eisenberg et al., 1980; Pate and Cooke, 1989), straining force-generating cross-bridges by lengthening of individual sarcomeres such as by external stretch might favor P_i binding and power stroke reversal. To test this, the effect of P_i on myofibrillar relaxation was investigated. Fig. 4 *A* shows that increasing $[P_i]$ from 0.2 to 5 mM reduced the cardiac myofibrillar force and increased k_{ACT} and k_{TR}, the rate constant of force redevelopment after a period of active unloaded shortening. This result is in accord with P_i reducing force by accelerating backward turnover kinetics of cross-bridges from force to non-force-generating states. The effects of $[P_i]$ on force transients after Ca^{2+} removal are shown in Fig. 4 *B*. The 5 mM P_i increased k_{LIN}, greatly shortened $t_{LIN,}$ and increased k_{REL}. The means of force and kinetic parameters at different $[P_i]$ are given in Table 1. The most P_i-sensitive parameter is t_{LIN}. It increases by $\sim$ 40% when P_i is reduced to 0.015 mM from the 0.2 mM contamination in our standard solutions by a P_i scavenging system. Thus, P_i, like stretch (Fig. 3), preinitiates the lengthening of the first sarcomere. At 5 mM P_i, k_{LIN} and k_{TR} are increased by similar amounts. Furthermore, high P_i increases k_{REL} and the rate of the sarcomeric propagation (latter not shown) by similar factors.

Previously we showed for cardiac myofibrils from various species that under maximum Ca^{2+} activations, k_{ACT} and k_{TR} are similar in value (Stehle et al., 2002). Table 1 also shows that k_{ACT} and k_{TR} are similarly affected by $[Ca^{2+}]$, temperature (T), and P_i. Whereas the value of k_{LIN} increases at higher (mM) $[P_i]$ and T, it is independent of the level of Ca^{2+} activation preceding relaxation. Comparing k_{LIN} and k_{REL} with k_{TR} reflecting Ca^{2+}-activated isometric cross-bridge turnover kinetics, $k_{LIN} < k_{TR} \ll k_{REL}$ under all conditions (Table 1) except at low partial Ca^{2+} activations where k_{TR} becomes similar to k_{LIN}.

DISCUSSION

Summary

Rapid, complete Ca^{2+} removal from isometrically held cardiac myofibrils induces two distinct relaxation phases. During the first phase isometric conditions are maintained in all sarcomeres and force decays with a rate constant (k_{LIN}) that is similar to the k_{TR} obtained at low Ca^{2+} activations, i.e., near relaxed conditions. This indicates that k_{LIN} predominantly reflects forward (g_{app}) and backward (f_{app}^{-}) turnover of cross-bridges from force to non-force-generating states with rate constants found under isometric conditions, and this also implies that the rate constant defining formation of force-generating cross-bridges (f_{app}) is down-regulated to relaxed-like steady-state values early after Ca^{2+} removal.

The second phase begins with the rapid lengthening of a single sarcomere indicating its mechanical relaxation. Interventions that favor the reversal of the cross-bridge power stroke (increasing cross-bridge strain or $[P_i]$) preinitiate this phase. Subsequent rapid sequential propagation of sarcomeric relaxation can be explained by an increase of f_{app}^{-} in

lengthening sarcomeres and an increase of g_{app} in shortening sarcomeres.

Force development kinetics

The rate constants of Ca^{2+}-induced myofibrillar force development (k_{ACT}) obtained here are similar to those of frog cardiac myofibrils (Colomo et al., 1998) and about two times higher than those reported previously for skinned trabeculae of the guinea pig (Palmer and Kentish, 1998). In line with previous findings on trabeculae (Palmer and Kentish, 1998), on rabbit psoas myofibrils (Colomo et al., 1998; Tesi et al., 2000), and on cardiac myofibrils of various species (Stehle et al., 2002), k_{ACT} is similar to the rate constant of force redevelopment (k_{TR}) after unloaded shortening at steady-state Ca^{2+} activation. Because k_{TR} is generally held to reflect isometric cross-bridge turnover kinetics (Brenner, 1988), this confirms previous interpretations (Palmer and Kentish, 1998; Colomo et al., 1998; Tesi et al., 2000; Stehle et al., 2002) that k_{ACT} is not limited by the Ca^{2+}-induced switch-on of the thin filament. The effects of Ca^{2+} and P_i on isometric force (F) and force (re)development kinetics (k_{TR} or k_{ACT}) given in Table 1 were fitted by a two-state model (Brenner, 1988):

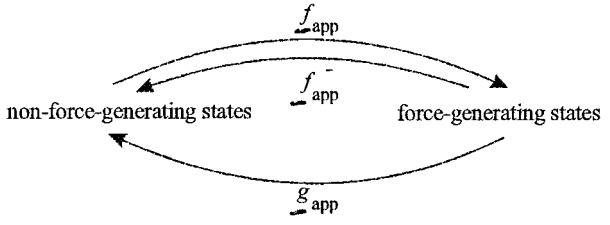

Based on this model, F is determined by cross-bridge turnover kinetics, i.e., $F \propto f_{app}/k_{TR}$ and $k_{TR} = k_{ACT} = f_{app} + g_{app} + f_{app}^-$, where Ca^{2+} regulates F only by modulating f_{app} (Brenner, 1988) and P_i reduces F only by increasing f_{app}^-. Defining $f_{app} = 1.0\ s^{-1}$ at maximum Ca^{2+} activation, $f_{app}^- = 0\ s^{-1}$ at 15 μM P_i, and $g_{app} = 0.5\ s^{-1}$, the theoretical k-F relation ($k = k_{TR} = k_{ACT}$) predicted by this simple model thereby never deviates more than 10% or 30% from the measured k_{ACT} or k_{TR} in Table 1, respectively. Such a rate modulation of F is in agreement with the dependences of k_{ACT} and k_{TR} on Ca^{2+} and P_i found in skinned cardiomyocytes (Araujo and Walker, 1994, 1996; Brandt et al., 1998; Tasche et al., 1999) and skinned trabeculae (Palmer and Kentish, 1998; Wolff et al., 1995).

Mechanism of myofibrillar relaxation

The key to understanding cross-bridge kinetics after complete Ca^{2+} removal is to relate the kinetics of each of the two phases of force decay to those of force redevelopment. In contrast to k_{TR}, k_{LIN} is independent of the activating [Ca^{2+}] and similar to the k_{TR} measured at low Ca^{2+} (Table 1), where the contribution of f_{app} to k_{TR} becomes negligible (Brenner, 1988). These results are consistent with two-state models (Huxley, 1957; Brenner, 1988) if we make the most simple assumptions that 1) f_{app} is rapidly reduced by fast, complete switch-off of the regulatory system after Ca^{2+} removal and 2) g_{app} and f_{app}^- do not change during the initial slow linear relaxation phase. Force should then decay with a rate constant $g_{app} + f_{app}^- = k_{TR} - f_{app}$ as predicted by force redevelopment kinetics. Indeed, subtracting $1.0\ s^{-1}$ (i.e., the value of f_{app} defined above to account for the increase in k_{TR} from low to high Ca^{2+}) from the k_{TR} determined at each [P_i] (Table 1) gives similar values to the obtained k_{LIN}. Together with the observation that sarcomeres remain isometric during the initial slow relaxation phase, this suggests that k_{LIN} reflects cross-bridge turnover kinetics determined by the same apparent rate constants (i.e., $g_{app} + f_{app}^-$) as during isometric force development near relaxed-like conditions.

Modeling reveals that any slow reduction of f_{app} would result in an initial lag phase during which force decreases at lower rates than after complete inhibition of cross-bridge reattachment. Kinetics observed with fluorescently labeled fast skeletal troponin incorporated into skinned rabbit psoas fibers (Brenner and Chalovich, 1999) and with cardiac troponin complex in vitro (Dong et al., 1996) yield off-rates of $15\ s^{-1}$ at 5°C and $20\ s^{-1}$ at 4°C, respectively. This should manifest in a lag with a $t_{1/2} \approx 20$ ms at 10°C in our force transients. The current resolution of the transients does not allow us to strictly confirm such a short lag at the beginning of the slow phase of force decay. Nevertheless, any transient maintenance of activation, whether arising from a slow switch-off of regulatory proteins or from feedback of force-generating cross-bridges, cannot account for the full period (up to 150 ms at low P_i) of the slow phase. High P_i and external stretches almost eliminate this phase, indicating that the tension shoulder at t_{LIN} is not due to cooperative thin filament inactivation, as also shown with skeletal myofibrils (Tesi et al., 2002). Instead, at this time the weakest sarcomere lengthens and myofibrillar force abruptly starts to decay with a 10–20 times faster rate (k_{REL}).

It is obvious from the sarcomere dynamics that take place during the rapid exponential force decay that k_{REL} cannot be taken as a direct parameter reflecting unique cross-bridge turnover kinetics in each sarcomere. Nevertheless, also to account for the fast propagation rate of sarcomere relaxation ($13 \pm 1\ s^{-1}$ per sarcomere, mean ± SE, evaluated from analysis of seven videos performed at standard conditions), cross-bridges must detach with apparent rate constants that are at least one order of magnitude higher than k_{LIN}. There is a need for a mechanism (relating cross-bridge kinetics to the current state of the sarcomere) that can explain 1) the

rapid relaxation of a single sarcomere, 2) the rapid propagation from one sarcomere to the next, and 3) the observed effects of stretch and P_i.

We propose that the following steps take place when relaxation propagates from one sarcomere to the next. 1) The weakest sarcomere starts to lengthen and residually attached cross-bridges become strained, whereupon they reverse the power stroke and detach (rate constant f_{app}^{-} becoming increased by strain). 2) The lengthening of the weak sarcomere reduces the strain in neighboring contracting sarcomeres, whereupon they actively shorten. 3) The shortening increases the apparent rate of forward transition of cross-bridges from force to non-force-generating states (g_{app}), inducing rapid cross-bridge detachment. 4) After some rapid detachment by forward kinetics, the remaining cross-bridges can no longer sustain the average load, and the shortening sarcomere turns to a weak sarcomere, thus becoming the next fully relaxed sarcomere (cf. step 1), and the cycle (steps 1–4) is repeated. Rapidity of cross-bridge detachment by both forward (cf. step 3) and backward (cf. step 1) turnover kinetics is required to account for the fast propagation from sarcomere to sarcomere. Cross-bridge models and kinetic evidence support these two pathways.

Faster cross-bridge detachment during active shortening of sarcomeres was first proposed by Huxley (1957). The rate constant for forward transition of cross-bridges from force to non-force-generating states can increase up to ~100 times at unloaded shortening (Stehle and Brenner, 2000). MgADP, which is known to strongly inhibit active shortening (Cooke and Pate, 1985), slows down relaxation kinetics in cardiac trabeculae (Simnett et al., 1998) and in skeletal myofibrils (Tesi et al., 2002). In cardiac myofibrils, the addition of 2 mM MgADP caused the propagation of sarcomeric relaxation to take frequent breaks between adjacent half-sarcomeres, thereby strongly reducing k_{REL} and the mean propagation rate both by a factor of 4 (unpublished data). However, it could be that activation by strongly bound cross-bridges also contributes to the slower relaxation at high [MgADP]. Lu et al. (2001) showed that in the presence of high [MgADP] strongly bound cross-bridges become formed that increase both Ca^{2+} sensitivity of force development and cross-bridge attachment rates. Maintenance of significant cross-bridge reattachment after Ca^{2+} removal at high [MgADP] would delay or slow down relaxation kinetics.

The acceleration of power stroke reversal by cross-bridge strain is thermodynamically consistent and predicted by models (Eisenberg et al., 1980; Pate and Cooke, 1989). Cross-bridge detachment by strain-induced power stroke reversal during lengthening of sarcomeres is consistent with small external stretches strongly shortening t_{LIN}. The stronger effect of P_i on t_{LIN} than on k_{REL} (see Table 1) is also in line with cross-bridge detachment mediated by P_i binding being most pronounced at high strain, i.e., when the force after Ca^{2+} removal is still high. Thus, in the sub-millimolar range, P_i seems only to affect the relaxation of the first or first few sarcomeres; nevertheless, in the physiological (millimolar) range it accelerates relaxation of most or all sarcomeres. High [P_i] had been also reported to increase the rate constant of the rapid exponential force decay observed after flash photolysis of the caged Ca^{2+} chelator diazo-2 in skinned cardiac trabeculae (Simnett et al., 1998). Interestingly, the values of k_{REL} and their dependence on [P_i] are similar to those of k_{Pi}, the rate constant of force decay after a step increase in [P_i] measured in cardiomyocytes (Araujo and Walker, 1996). k_{Pi} is thought to probe the kinetics of the power stroke reversal (Millar and Homsher, 1990; Araujo and Walker, 1996; Tesi et al., 2000). The similarity of k_{Pi} and k_{REL} therefore suggests that the pathway probed by k_{Pi} is sufficiently fast to take place during the rapid relaxation phase.

To summarize, during the rapid relaxation phase, within an individual shortening sarcomere, cross-bridges detach by more rapid forward turnover kinetics than under isometric conditions; and then, while the sarcomere is lengthening, cross-bridges detach by more rapid backward turnover kinetics than under isometric conditions. One intriguing conclusion from this mechanism is that the free energy intrinsic to a myofibril can be partly conserved. The elastic energy provided by cross-bridges in shortening sarcomeres is transferred by the filaments to the lengthening sarcomeres, thus favoring cross-bridges to resume an ADP·P_i state. This enables them to perform a power stroke at the next activation without using fresh ATP.

Although the present study provides evidence for the first time that sarcomeres relax sequentially, organized sarcomere behavior is also found under steady-state conditions. Spontaneous oscillatory contractions (SPOCs), indicated by oscillations of force and individual SL, had been observed in cardiac myofibrils under partial Ca^{2+} activations (Linke et al., 1993). Ishiwata's group found SPOCs in single skeletal myofibrils (Anazawa et al., 1992; Shimizu et al., 1992) and skinned cardiac fibers (Fukuda and Ishiwata, 1999) also to occur in the absence of Ca^{2+} on condition that ADP and P_i were present. They also showed that SPOCs take place even in the absence of regulatory proteins, indicating that the occurrence of SPOCs is a phenomenon inherent to the actomyosin motor itself (Fujita and Ishiwata, 1998). Therefore, it is likely that SPOCs and the propagation of relaxation along the sarcomeres in a myofibril, which (as argued above) occurs after the thin filament is already turned off, result from the same intersarcomere chemomechanical coupling mechanism and are not based on any regulatory processes.

Extrapolation to relaxation kinetics in fibers

In myofibrils from fast skeletal muscle, similar clear-cut biphasic force relaxation transients, as found here in cardiac myofibrils with a similar ratio of $k_{LIN}/k_{REL} \approx 1/20$, have

been observed (Tesi et al., 2002). Initial, slow, linear force decays preceding a rapid exponential phase had been found also in photolysis studies in skinned fast skeletal muscle fibers (Rall and Wahr, 1998; Hoskins et al., 1999), but transients are less markedly biphasic ($k_{LIN}/k_{REL} \approx 1/3$) and exhibit less pronounced tension shoulders than in myofibrils. The rate constants of the rapid relaxation phase found in all photolysis studies in skinned guinea pig trabeculae (10–12 s^{-1} at 12°C (Johns et al., 1997, 1999; Simnett et al., 1998)) except for one (3 s^{-1} at 22°C (Palmer and Kentish, 1998)) are similar to the k_{REL} (11 s^{-1} at 10°C) in our study. However, a pronounced initial slow phase, as found here with cardiac myofibrils, was not found in any of the studies on skinned cardiac trabeculae (Zhang et al., 1995; Palmer and Kentish, 1997, 1998; Simnett et al., 1998; Fitzsimons et al., 1998; Johns et al., 1997, 1998, 1999; Kentish et al., 2001). Technical reasons probably account for these differences: 1) the thicker the fiber, the more P_i will accumulate during the preceding contraction and then prematurely initiate the rapid relaxation phase; 2) because of the larger number of sarcomeres in series in fibers, lengthening might start at multiple sarcomeres and result in less sharp tension shoulders; and 3) in myofibrils and skeletal muscle fibers, sarcomeres are unidirectionally arranged, whereas in the multicellular trabeculae, sarcomeres are less uniformly orientated, and this might produce additional sarcomere inhomogeneity during contraction and preinitiate rapid nonisometric relaxation.

Laser diffraction on segments of living frog skeletal muscle fibers revealed large, erratic changes in mean SL (2–4% shortening, 6–12% lengthening, or simultaneous lengthening and shortening indicated by splitting of the first-order diffraction peak) during post-tetanic relaxation (Edman and Flitney, 1982). Changes in mean SL (Edman and Flitney, 1982) or segmental fiber length (Huxley and Simmons, 1970) thereby invariably begin at the onset of the final rapid exponential tension decay, in temporal correlation with the lengthening of the first sarcomere in the myofibril. After the photorelease of caged Ca^{2+} chelators in skinned skeletal muscle fibers, smaller changes in mean SL ($\pm$1.5%) had been observed (Hoskins et al., 1999) than in living fibers. It has been argued that the changes in living fibers result from inhomogeneous reuptake of Ca^{2+} into the sarcoplasmic reticulum and that the SL changes persisting in skinned fibers do not alter cross-bridge turnover kinetics (Hoskins et al., 1999). The present results challenge these conclusions. As shown (Fig. 3 *B*), stretches of 0.6% in myofibril length halve t_{LIN}. It is a matter of pure statistics that the mean SL will greatly underestimate the maximum length changes of individual sarcomeres, especially if only a small fraction of sarcomeres lengthens as during the beginning of the rapid force decay. The mean SL would be little affected during whole relaxation, if the lengthening of relaxed sarcomeres is compensated by the shortening of contracting sarcomeres. Major changes in the mean SL will probably be detected at maximum overall variance in SL, i.e., when approximately half of all sarcomeres become lengthened. This takes place in cardiac myofibrils when force drops to 3–5% of its initial value (Fig. 1 *B*), in temporal correlation with mean SL changes in living fibers, passing a maximum when force approaches zero (Huxley and Simmons, 1970; Edman and Flitney, 1982). It is thus possible that the sarcomere behavior described here occurs in vivo.

In conclusion, sarcomere dynamics during striated muscle relaxation should not be dismissed as inhomogeneous. Instead, it appears to be a highly organized process that combines prospective benefits for muscle function: intersarcomeric chemomechanical coupling increasing the energetic efficiency during a contraction-relaxation cycle and at the same time accelerating mechanical relaxation. Rapid relaxation of myofibrils is likely of physiological significance in the heart to improve its diastolic function.

We are grateful to Corrado Poggesi (University Florence) and Phil. W. Brandt (Columbia) for many stimulating discussions and helpful comments on the manuscript.

This work was supported by grants from Köln Fortune (Faculty of Medicine, Cologne) to R.S.

REFERENCES

Anazawa, T., K. Yasuda, and S. Ishiwata. 1992. Spontaneous oscillation of tension and sarcomere length in skeletal myofibrils: microscopic measurement and analysis. *Biophys. J.* 61:1099–1108.

Araujo, A., and J. W. Walker. 1994. Kinetics of tension development in skinned cardiac myocytes measured by photorelease of Ca^{2+}. *Am. J. Physiol.* 267:H1643–H1653.

Araujo, A., and J. W. Walker. 1996. Phosphate release and force generation in cardiac myocytes investigated with caged phosphate and caged calcium. *Biophys. J.* 70:2316–2326.

Brandt, P. W., F. Colomo, N. Piroddi, C. Poggesi, and C. Tesi. 1998. Force regulation by Ca^{2+} in skinned single cardiac myocytes of frog. *Biophys. J.* 74:1994–2004.

Brenner, B. 1988. Effect of Ca^{2+} on cross-bridge turnover kinetics in skinned single rabbit psoas fibers: implications for regulation of muscle contraction. *Proc. Natl. Acad. Sci. U.S.A.* 85:3265–3269.

Brenner, B., and J. M. Chalovich. 1999. Kinetics of thin filament activation probed by fluorescence of *N*-((2-(iodoacetoxy)ethyl)-*N*-methyl)amino-7-nitrobenz-2-oxa-1,3-diazole-labeled troponin I incorporated into skinned fibers of rabbit psoas muscle: implications for regulation of muscle contraction. *Biophys. J.* 77:2692–2708.

Cecchi, G., F. Colomo, C. Poggesi, and C. Tesi. 1993. A force transducer and a length-ramp generator for mechanical investigations of frog-heart myocytes. *Pflugers Arch.* 423:113–120.

Colomo, F., S. Nencini, N. Piroddi, C. Poggesi, and C. Tesi. 1998. Calcium dependence of the apparent rate of force generation in single striated muscle myofibrils activated by rapid solution changes. *Adv. Exp. Med. Biol.* 453:373–381.

Colomo, F., N. Piroddi, C. Poggesi, K. te Kronnie, and C. Tesi. 1997. Active and passive forces of isolated myofibrils from cardiac and fast skeletal muscle of the frog. *J. Physiol. (Lond.).* 500:535–548.

Cooke, R., and E. Pate. 1985. The effects of ADP and phosphate on the contraction of muscle fibers. *Biophys. J.* 48:789–798.

Dong, W., S. S. Rosenfeld, C. K. Wang, A. M. Gordon, and H. C. Cheung. 1996. Kinetic studies of calcium binding to the regulatory site of troponin C from cardiac muscle. *J. Biol. Chem.* 271:688–694.

Edman, K. A., and F. W. Flitney. 1982. Laser diffraction studies of sarcomere dynamics during 'isometric' relaxation in isolated muscle fibres of the frog. *J. Physiol. (Lond.).* 329:1–20.

Eisenberg, E., T. L. Hill, and Y. Chen. 1980. Cross-bridge model of muscle contraction: quantitative analysis. *Biophys. J.* 29:195–227.

Fearn, L. A., M. L. Bartoo, J. A. Myers, and G. H. Pollack. 1993. An optical fiber transducer for single myofibril force measurement. *IEEE Trans. Biomed. Eng.* 40:1127–1132.

Fitzsimons, D. P., J. R. Patel, and R. L. Moss. 1998. Role of myosin heavy chain composition in kinetics of force development and relaxation in rat myocardium. *J. Physiol. (Lond.).* 513:171–183.

Fujita, H., and S. Ishiwata. 1998. Spontaneous oscillatory contraction without regulatory proteins in actin filament-reconstituted fibers. *Biophys. J.* 75:1439–1445.

Fukuda, N., and S. Ishiwata. 1999. Effects of pH on spontaneous tension oscillation in skinned bovine cardiac muscle. *Pflugers Arch.* 438: 125–132.

Hoskins, B. K., S. Lipscomb, I. P. Mulligan, and C. C. Ashley. 1999. How do skinned skeletal muscle fibers relax? *Biochem. Biophys. Res. Commun.* 254:330–333.

Huxley, A. F. 1957. Muscle structure and theories of contraction. *Prog. Biophys. Chem.* 27:255–318.

Huxley, A. F., and R. M. Simmons. 1970. Rapid 'give' and the tension 'shoulder' in the relaxation of frog muscle fibres. *J. Physiol.* 210: 32P–33P.

Johns, E. C., E. A. Hodson, H. Fish, J. S. Lymn, H. Thurston, I. P. Mulligan, and C. C. Ashley. 1998. Investigating the relaxation, following diazo-2 laser flash photolysis, of a skinned trabecular preparation from SHR hypertrophied left ventricle. *Pflugers Arch.* 436:155–158.

Johns, E. C., K. O. Ryder, E. A. Hodson, G. Hart, I. P. Mulligan, S. Lipscomb, and C. C. Ashley. 1999. Investigating the relaxation rate, following diazo-2 photolysis, of a skinned trabecular preparation from guinea-pig hypertrophied left ventricle. *Pflugers Arch.* 438:771–777.

Johns, E. C., S. J. Simnett, I. P. Mulligan, and C. C. Ashley. 1997. Troponin I phosphorylation does not increase the rate of relaxation following laser flash photolysis of diazo-2 in guinea-pig skinned trabeculae. *Pflugers Arch.* 433:842–844.

Kentish, J. C., D. T. McCloskey, J. Layland, S. Palmer, J. M. Leiden, A. F. Martin, and R. J. Solaro. 2001. Phosphorylation of troponin I by protein kinase A accelerates relaxation and crossbridge cycle kinetics in mouse ventricular muscle. *Circ. Res.* 88:1059–1065.

Linke, W. A., M. L. Bartoo, and G. H. Pollack. 1993. Spontaneous sarcomeric oscillations at intermediate activation levels in single isolated cardiac myofibrils. *Circ. Res.* 73:724–734.

Linke, W. A., V. I. Popov, and G. H. Pollack. 1994. Passive and active tension in single cardiac myofibrils. *Biophys. J.* 67:782–792.

Lu, Z., Swartz, D. R., Metzger, J. M., Moss, R. L., and J. W. Walker. 2001. Regulation of force development studied by photolysis of caged ADP in rabbit skinned psoas fibers. *Biophys. J.* 81:334–344.

Millar, N. C., and E. Homsher. 1990. The effect of phosphate and calcium on force generation in glycerinated rabbit skeletal muscle fibers: a steady-state and transient kinetic study. *J. Biol. Chem.* 265: 20234–20240.

Palmer, S., and J. C. Kentish. 1997. Differential effects of the Ca^{2+} sensitizers caffeine and CGP 48506 on the relaxation rate of rat skinned cardiac trabeculae. *Circ. Res.* 80:682–687.

Palmer, S., and J. C. Kentish. 1998. Roles of Ca^{2+} and cross-bridge kinetics in determining the maximum rates of Ca^{2+} activation and relaxation in rat and guinea pig skinned trabeculae. *Circ. Res.* 83: 179–186.

Pate, E., and R. Cooke. 1989. A model of cross-bridge action: the effects of ATP, ADP and Pi. *J. Muscle Res. Cell Motil.* 10:181–196.

Piazzesi, G., M. Linari, M. Reconditi, F. Vanzi, and V. Lombardi. 1997. Cross-bridge detachment and attachment following a step stretch imposed on active single frog muscle fibres. *J. Physiol. (Lond.).* 498:3–15.

Rall, J. A., and P. A. Wahr. 1998. Role of calcium and cross-bridges in modulation of rates of force development and relaxation in skinned muscle fibers. *Adv. Exp. Med. Biol.* 453:219–227.

Rayment, I., H. M. Holden, M. Whittaker, C. B. Yohn, M. Lorenz, K. C. Holmes, and R. A. Milligan. 1993. Structure of the actin-myosin complex and its implications for muscle contraction. *Science.* 261:58–65.

Shimizu, H., T. Fujita, and S. Ishiwata. 1992. Regulation of tension development by MgADP and P_i without Ca^{2+}: role in spontaneous tension oscillation of skeletal muscle. *Biophys. J.* 61:1087–1098.

Simnett, S. J., E. C. Johns, S. Lipscomb, I. P. Mulligan, and C. C. Ashley. 1998. Effect of pH, phosphate, and ADP on relaxation of myocardium after photolysis of diazo 2. *Am. J. Physiol.* 275:H951–H960.

Stehle, R., and B. Brenner. 2000. Cross-bridge attachment during high-speed active shortening of skinned fibers of the rabbit psoas muscle: implications for cross-bridge action during maximum velocity of filament sliding. *Biophys. J.* 78:1458–1473.

Stehle, R., M. Kruger, and G. Pfitzer. 2002. Isometric force kinetics upon rapid activation and relaxation of mouse, guinea pig, and human heart muscle studied on the subcellular myofibrillar level. *Basic Res. Cardiol.* 97:I/127–I/135.

Tasche, C., E. Meyhofer, and B. Brenner. 1999. A force transducer for measuring mechanical properties of single cardiac myocytes. *Am. J. Physiol.* 277:H2400–H2408.

Tesi, C., F. Colomo, S. Nencini, N. Piroddi, and C. Poggesi. 2000. The effect of inorganic phosphate on force generation in single myofibrils from rabbit skeletal muscle. *Biophys. J.* 78:3081–3092.

Tesi, C., N. Piroddi, F. Colomo, and C. Poggesi. 2002. Relaxation Kinetics Following Sudden Ca^{2+} Reduction in Single Myofibrils from Skeletal Muscle. *Biophys. J.* 83:2142–2151.

Wolff, M. R., K. S. McDonald, and R. L. Moss. 1995. Rate of tension development in cardiac muscle varies with level of activator calcium. *Circ. Res.* 76:154–160.

Zhang, R., J. Zhao, A. Mandveno, and J. D. Potter. 1995. Cardiac troponin I phosphorylation increases the rate of cardiac muscle relaxation. *Circ. Res.* 76:1028–1035.